Air Shower Simulation Results With the Latest Generation of High Energy Hadronic Interaction Models

T. Pierog, R. Engel, and D. Heck
Institut für Kernphysik
Forschungszentrum Karlsruhe
Karlsruhe, Germany
Email: tanguy.pierog@ik.fzk.de

S.S. Ostapchenko
IEKP
Universität Karlsruhe
Karlsruhe, Germany

K. Werner
SUBATECH
Nantes, France

***Abstract*— Interpretation of EAS experimental results is strongly based on air shower simulations. The latter being based on hadronic interaction models, any new model can help for the understanding of the nature of cosmic rays. The new models QGSJET-II and EPOS reproducing all major results of existing accelerator data (including detailed data of RHIC experiments for EPOS) have been introduced in air shower simulation programs CORSIKA and CONEX allowing comparison with former models such as QGSJET01 or SIBYLL. Results for air shower observables will be discussed in details.**

I. Introduction

Since almost one century, physicists study characteristics of cosmic rays. Because of the very steep energy spectrum of the primary particles, direct detection by satellite or balloon flight can only be done up to $\sim 10^{14}$ eV, where approximatively only one particle/m^2/s reaches the Earth. Fortunately, it is at this energy that the cascade of particles produced by the primary particle reaches the ground. This is called extended air shower (EAS) and is used to make indirect measurements of high energy cosmic rays. The upper limit of the detectable energy is then given by the area of the detector. For instance, the Pierre AUGER Observatory [1], being built in Argentina, detects particles above $\sim 10^{20}$ eV for which the flux should be much less than one particle per km^2 and century.

Air showers can be observed by different ways. The simplest is to detect secondary particles reaching the ground. Using an array of particle detectors (for γ, electrons and μ), the geometry, the mass, and the energy of the primary cosmic ray particle can be reconstructed. In particular, each shower will be characterized by its lateral distribution function (LDF). For energies above $\sim 10^{17}$ eV, the longitudinal profile of a shower can be directly observed by the fluorescence light emitted. Two main observables can be extracted : $N_{\max}$, the number of particles at the maximum, and $X_{\max}$ the position (in slant depth, quantity of matter crossed by particles along the shower axis) of this maximum. As we will see in the following, these quantities can be used to estimate the energy and mass of the primary particles. Shower-to-shower fluctuations of all this observables are also useful informations.

As a consequence, one needs an accurate simulation of air showers to extract information on the primary particle, such as its energy or mass, from the observation of secondary particles. The primary particle being a proton or a nucleus as observed by direct measurement at low energy, the first interaction starting the shower is a hadronic interaction (like in collider experiment). Each hadronic interaction produces secondary particles ; neutral pions will decay into photons which will initiate electromagnetic sub-showers. As a consequence, all major results of EAS simulation will rely on the hadronic interaction model giving the nature, yield and energy spectra of all hadronic secondary particles. In particular, the energy spectrum of secondary neutral pions is very important for the energy transfer to the electromagnetic component of the EAS.

Since more than half a decade, mostly two hadronic models are used in EAS simulations, namely SIBYLL 2.1 [2] and QGSJET01 [3]. Both of them are based on the same kind of physics, taking care of multiple scattering but neglecting screening type effects at high energy. These are fast models which are supposed to describe basic observables of hadronic interactions needed for EAS simulations. In 2006, two new models were included in EAS simulation codes such as CORSIKA [4] or CONEX [5] used in this analysis : QGSJET II-3 [6] and EPOS [7]. In section II, the basic ideas of these models will be exposed. Results compared with accelerator data will be shown in section III for hadronic interactions and results for EAS simulation will be presented section IV.

II. Model Description

A. QGSJET II-3

The QGSJET-II model, being based on the Pomeron phenomenology [8], describes hadronic multiple scattering processes as multiple exchanges of composite objects corresponding to independent microscopic parton cascades. For the soft low virtuality cascades a phenomenological 'soft' Pomeron amplitude is employed, whereas semi-hard scattering processes are treated as exchanges of 'semi-hard Pomerons', the latter composed of a piece of QCD parton ladder 'sandwiched' between two soft Pomerons [9], [10]; the soft Pomerons

and the ladder describing correspondingly the low and high virtuality parts of the underlying parton cascade. The principal feature of QGSJET-II is the treatment of non-linear parton effects described as Pomeron-Pomeron interactions, based on all order re-summation of the corresponding Reggeon Field Theory diagrams [6], [11]. The basic assumption of the scheme is that Pomeron-Pomeron coupling is dominated by non-perturbative parton processes and can be described by means of phenomenological multi-Pomeron vertices. The approach allows one to obtain a consistent description of various hadronic cross sections and structure functions, including diffractive ones, for a fixed, energy-independent cutoff [6] between soft and hard parton evolution. Presently it is the most advanced model for the description of hadronic interactions in the peripheral and the 'transition' regimes. However, in central collisions one may expect sizable corrections to come from 'hard' (high q^2) Pomeron-Pomeron coupling, which is neglected in QGSJET-II. A reasonable agreement of the model predictions for central nucleus-nucleus collisions with the data of RHIC collider indicates the smallness of such effects [12]. Nevertheless, the situation may change at much higher energies.

B. EPOS

The EPOS model, being the successor to NEXUS [13], employs the above-discussed soft and semi-hard Pomeron scheme and, in contrast to all other MC generators, takes into account energy-momentum correlations between multiple re-scatterings [14] (see also [15] for a qualitative discussion). The description of non-linear effects is based on an effective treatment of lowest order Pomeron-Pomeron interaction graphs, with the corresponding parameters being adjusted from comparison with RHIC data [7]. A big advantage of the model is an excellent calibration to available accelerator data. Its extrapolation towards very high energies may depend on the adopted empirical parameterizations for non-linear interaction contributions, but since the non-linear effects are both energy and mass dependent (increasing the mass of the projectile or target is like increasing the energy), collisions of Deuteron projectile on Gold target at 200 GeV center-of-mass is equivalent of a proton-Air interaction at 10^{20} eV primary energy. A saturation effect being already needed to describe RHIC data, the extrapolation of non-linear effects in EPOS are quite safe even at ultra-high energy. Another important original aspect of EPOS is that all Pomerons are treated in the same way [16]. There is not a first Pomeron connected to the valence quarks and then secondary Pomerons like in the usual scheme, but all Pomerons are equivalent and usually connected to sea quarks. The valence quarks stay most of the time in the projectile and target remnant, and these remnant objects are hadronized independently. As a result, it allows a much better description of baryon and anti-baryon production as shown in section III-A. Furthermore, EPOS is the only model of this analysis which is not only used for cosmic ray physics, but is used in heavy ion physic to describe SPS and RHIC data. This constraint implies a very good description of much more observables than usually taken into account for air shower simulations and especially for baryon-antibaryon production.

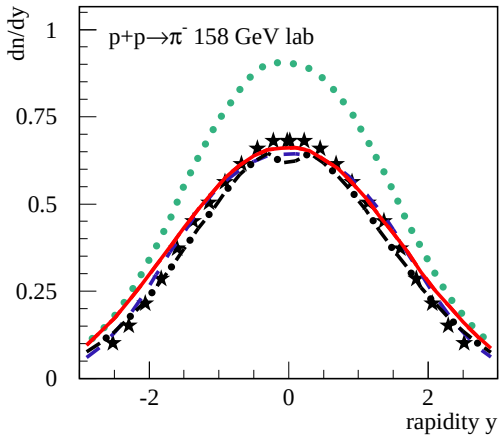

Fig. 1. Rapidity distribution of negative pions produced by a 158 GeV proton beam on a proton target. Simulations with QGSJET-II (full red line), EPOS (dashed blue line), QGSJET01 (dotted green line) and SIBYLL2.1 (dashed-dotted black line) are shown together with data from NA49 experiment [17] (stars).

III. Results for Hadronic Interactions

Results of simulation with QGSJET-II and EPOS 1.55 will be shown together with QGSJET01 and SIBYLL2.1 as a reference (when possible). They will be compared to accelerator data and all the simulations are done with the same triggers for all models and as close as possible to the experimental conditions.

A. Low Energy

In this subsection, we consider only data from fixed target experiments. Hence the energy is given in the laboratory system. Proton-proton collision will be considered first. It is a good benchmark because of the quality and quantity of the data, even if it is not what happens in air shower development. The first thing to notice is that except for QGSJET01 which has a well-known problem with the multiplicity at low energy, the overall description of basic distributions such as rapidity distributions is very good for all models. As an example, the rapidity distribution of negative pions produced at 158 GeV by all the models and compared to NA49 data is shown in Fig.1.

Looking more into details, the situation appears to be quite different from one model to another. In Fig.2, it is clearly shown that all models except EPOS fail to describe the Lambda rapidity distribution at 158 GeV from NA49 experiment. As already explained, this is due to a special treatment of the remnant fragmentation in EPOS which play a fundamental role at low energy and in the forward region which is very important for air shower simulations.

On the Longitudinal momentum fraction x distribution of protons produced in 100 GeV collisions as measured by the

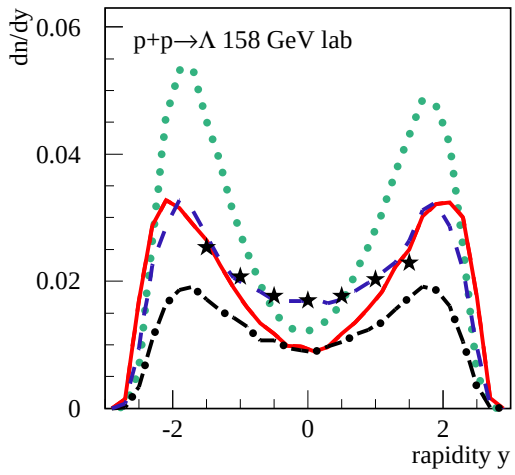

Fig. 2. Rapidity distribution of Lambdas produced by a 158 GeV proton beam on a proton target. Simulations with QGSJET-II (full red line), EPOS (dashed blue line), QGSJET01 (dotted green line) and SIBYLL2.1 (dashed-dotted black line) are shown together with data from NA49 experiment [18] (stars).

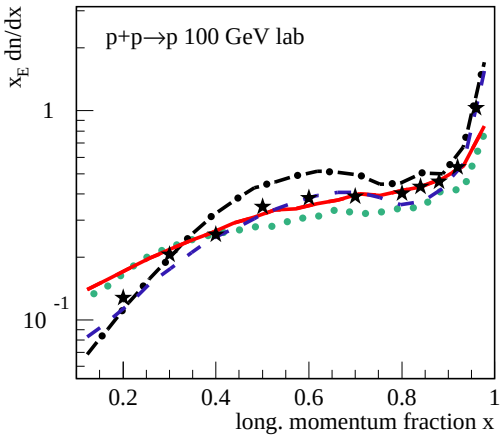

Fig. 3. Longitudinal momentum fraction x of protons produced by a 100 GeV proton beam on a proton target. Simulations with QGSJET-II (full red line), EPOS (dashed blue line), QGSJET01 (dotted green line) and SIBYLL2.1 (dashed-dotted black line) are shown together with data from FNAL-E-0118 experiment [19] (stars).

FNAL-E-0118 experiment and shown in Fig.3, one can easily notice the differences between hadronic interaction models. They all present a diffractive peak at large x, but in this region very important for air shower development, the difference between QGSJET01 and SIBYLL can be as large as a factor of 2. The difference between QGSJET-II and EPOS is a bit less pronounced but real.

Changing to a more realistic system for air-showers like a proton or pion beam on a Carbon target, we can conclude the same. Basic observables like rapidity distributions for negative pions as shown Fig.4 with NA49 data, are well reproduced. But on a more specific distribution like the longitudinal momentum distribution of protons and antiprotons produced by a 100 GeV positive pion beam on a Carbon target from FNAL-E-0118 experiment [21] , Fig.5, we can see that again only EPOS is able to reproduce these data. The SIBYLL spectrum is too hard, and QGSJET-II spectrum is too low by a factor of 2 (even more for QGSJET01). This is a very important reaction in air shower, and baryon pair production is in particular important for muon production as discussed in [22] and more recently in [23].

At this stage, it is important to notice that distributions shown here are second order corrections for air shower simulations. It is important to keep in mind, that the first order (rapidity distributions, multiplicity distributions, elasticity, mean pt) is well reproduced by all the models, including the 'old' generation. But it can have some impact on details of the air shower development, such as the muon number.

B. High Energy

Going to collider experiments, the energy is now expressed in the center-of-mass system. It corresponds to the typical

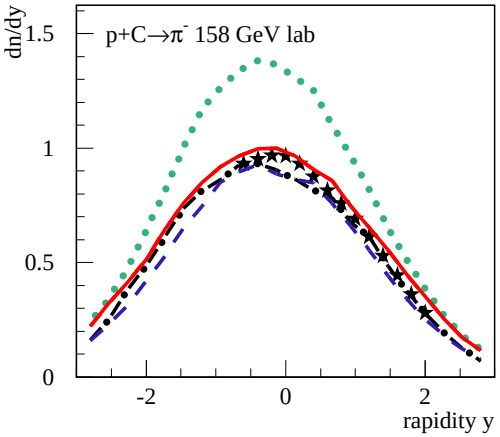

Fig. 4. Rapidity distribution of negative pions produced by a 158 GeV proton beam on a Carbon target. Simulations with QGSJET-II (full red line), EPOS (dashed blue line), QGSJET01 (dotted green line) and SIBYLL2.1 (dashed-dotted black line) are shown together with data from NA49 experiment [20] (stars).

energy of hadronic interactions in air showers. Unfortunately, the data are mostly available for the secondary particles produced in the central region of the reaction and not for the leading particles important for the air showers.

Again, the main distributions such as the pseudo-rapidity distributions, Fig.6, or transverse momentum distributions, Fig.7, are very well reproduced by hadronic interaction models for proton-antiproton collisions.

But thanks to the RHIC collider, new data are now available with a very high quality and heavier system such as for the Deuteron-Gold interaction. This allows us to test higher order

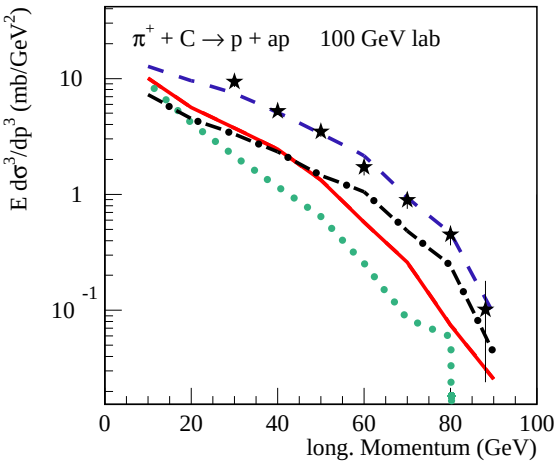

Fig. 5. Longitudinal momentum distribution of protons and antiprotons produced by a 100 GeV positive pion beam on a Carbon target. Simulations with QGSJET-II (full red line), EPOS (dashed blue line), QGSJET01 (dotted green line) and SIBYLL2.1 (dashed-dotted black line) are shown together with data from FNAL-E-0118 experiment [21] (stars).

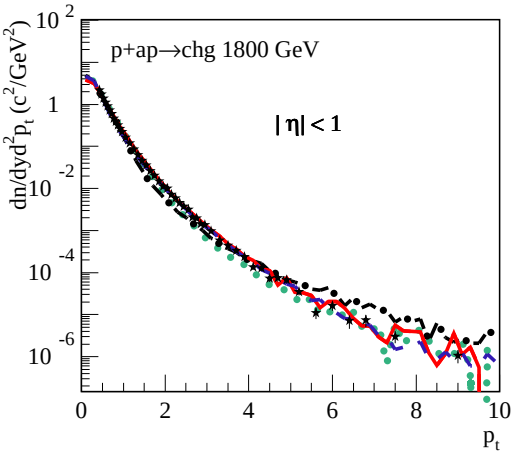

Fig. 7. Transverse momentum distribution of charged particles at mid-pseudo-rapidity produced by proton-proton collision at 1800 GeV center-of-mass energy. Simulations with QGSJET-II (full red line), EPOS (dashed blue line), QGSJET01 (dotted green line) and SIBYLL2.1 (dashed-dotted black line) are shown together with data from E775 experiment [25] (stars).

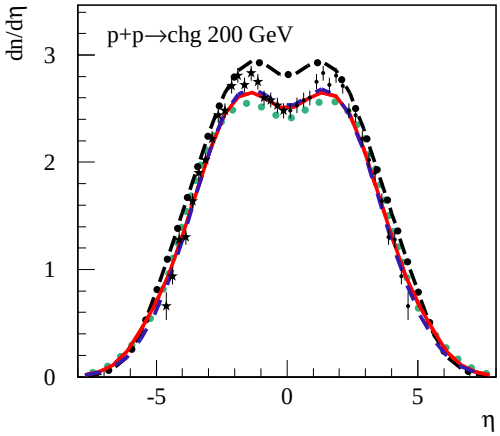

Fig. 6. Pseudo-rapidity distribution of charged particles produced by proton-proton collision at 200 GeV center-of-mass energy. Simulations with QGSJET-II (full red line), EPOS (dashed blue line), QGSJET01 (dotted green line) and SIBYLL2.1 (dashed-dotted black line) are shown together with data from UA5 experiment [24] (stars).

effects which are not included in QGSJET01 or SIBYLL, but are the main improvement for QGSJET-II and EPOS. Comparing QGSJET-II to RHIC data makes clear the point that the extrapolation from proton-proton collision is not straight forward. Even if non-linear effects are taken into account, QGSJET-II underestimates multiplicity of central collisions (Fig.8) and does not show any p_t enhancement. Indeed Fig.9 shows one of the main results of RHIC experiments. From theory, we expect that the number of high transverse momentum (p_t) particles produced in central D-Au interactions should scale like the number of binary collisions times the number of particles produced with the same p_t in pp interactions. But it is not the case in central collision and in particular for heavy particles like baryons/antibaryons as shown Fig.9 for protons and antiprotons. The data measured by STAR experiment [28] are clearly above the theoretical expectation of 1 (thin line) for the ration D-Au over pp.

In EPOS, string fragmentation is modified by a 'measure' of the energy density of the medium [7] to take into account the observed effect. It is the reason why EPOS does reproduce this data. But it is worth to notice that there is no special modification of the EPOS theoretical scheme to get the pseudo-rapidity right as shown in Fig.8.

C. Extrapolation

As seen in previous subsections, all models agree well with data on the main observables, and usually disagree on more specific data either not yet known when the model was build or not considered as important for air shower development (such as high p_t particles or rare baryons). These hadronic models being used for ultra-high energy cosmic rays whose energy is well above the maximum energy used in collider experiment, it is important to compare results in a domain where no data are available.

First of all, simulations can be compared at LHC energy for which data should be available in the next few years. The pseudo-rapidity distribution of charged particles produced by proton-Carbon collisions at 14 TeV is shown in Fig.10. At this energy, there is already a 25% difference on the plateau height between QGSJET-II and EPOS predictions. So after only one order of magnitude in energy, the differences between the models become significant even for the main observables.

Looking at the evolution of the multiplicity of secondary particles produced in central region of proton-air interaction

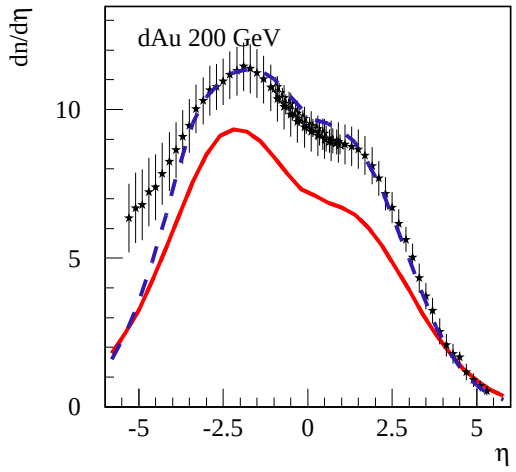

Fig. 8. Pseudo-rapidity distribution of hadrons produced at mid-rapidity by minimum-biased Deuteron-Gold collisions at 200 GeV center-of-mass energy over the one produced by proton-proton collision in the same conditions and scaled by the number of binary collisions. Simulations with QGSJET-II (full red line) and EPOS (dashed blue line), are shown together with data from STAR [26] and PHOBOS [27] experiments (stars)

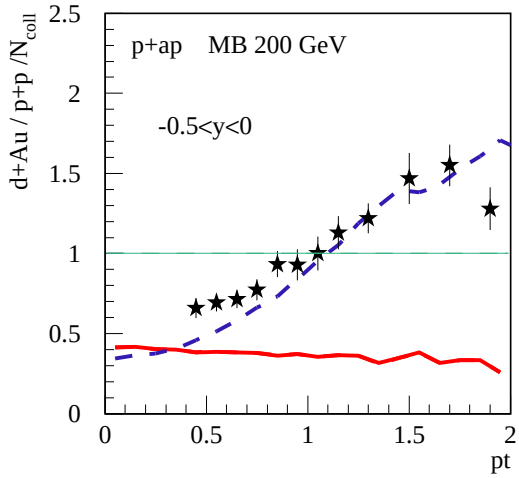

Fig. 9. Transverse momentum distribution of proton and antiproton at mid-rapidity produced by minimum-biased Deuteron-Gold collisions at 200 GeV center-of-mass energy over the one produced by proton-proton collision in the same conditions and scaled by the number of binary collisions. Simulations with QGSJET-II (full red line) and EPOS (dashed blue line), are shown together with data from STAR experiment [28] (stars)

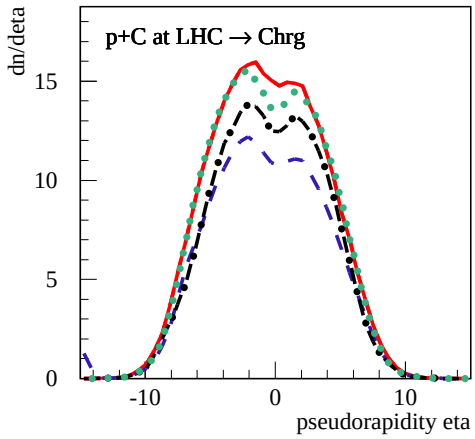

Fig. 10. Pseudo-rapidity distribution of charged particles produced by proton-Carbon collisions at 14000 GeV center-of-mass energy. Simulations with QGSJET-II (full red line), EPOS (dashed blue line), QGSJET01 (dotted green line) and SIBYLL2.1 (dashed-dotted black line) are shown.

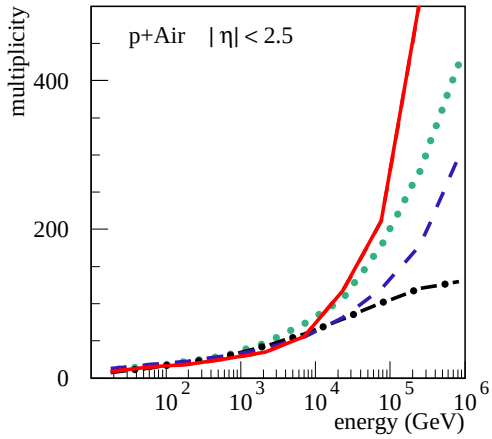

Fig. 11. Multiplicity of charged particles produced in proton-Air interactions at mid-pseudo-rapidity as a function of the nucleon pair center-of-mass energy in GeV. Simulations with QGSJET-II (full red line), EPOS (dashed blue line), QGSJET01 (dotted green line) and SIBYLL2.1 (dashed-dotted black line) are shown.

as a function of the collision energy Fig.11, the different extrapolation of the models appears clearly. Up to a few TeV, where data exists, all models predict almost the same number of secondary particles, but then the multiplicity increases very quickly for QGSJET01 or QGSJET-II while SIBYLL has a very slow increase and EPOS is in between. At the highest energy, QGSJET-II gives more than 5 times more particles than SIBYLL.

IV. Results for Air Showers

In fact, these very different extrapolations do not really show up in air shower simulations. Indeed the very high multiplicity in QGSJET is given by very slow particles which do not

play a big role in air shower development. The latter being correlated with very fundamental quantities such as the cross section, the inelasticity or the multiplicity of fast particles [29] which are not so different from one model to another. In the following, simulation were performed with CONEX with an incident angle of 60^o and where the minimum energy for the muons is 1 GeV and 1 MeV for electrons and positrons.

A. Elongation rate

As an illustration, the mean shower development maximum ($< X_{\max} >$) for all the models is presented Fig.12 for the highest energy. Below 10^{19} eV, all the models agree within 20 g/cm^2 for proton induced showers. In this domain, $< X_{\max} >$ of QGSJET-II is shifted towards higher value compared to QGSJET01, but for the highest energy, the two models agree. As a consequence, around 10^{18} eV an analysis of $< X_{\max} >$ based on QGSJET-II will predict higher cosmic ray primary mass than with QGSJET01, close to SIBYLL results. At low energy, despite quite different predictions for the hadronic interactions, EPOS $< X_{\max} >$ is very close to QGSJET01 result. However above 10^{19} eV, results of EPOS for proton induced shower are closer to SIBYLL one, and predict even deeper shower maxima. This is due to a different elongation rate for EPOS compared to all other models, approximatively 5 g/cm^2/decade more than QGSJET01, QGSJET-II or SIBYLL and is correlated to the next result: the number of muons produced in an air shower.

B. Muon Content

One of the most important component to study the primary cosmic ray mass composition is the number of muons reaching the ground and its correlation with the number of charged particles. In Fig.13, the contour plot giving half the probability to have a given combination of a number of muons and a number of charged particles per shower is shown for 10^{15}, 10^{16}, 10^{17} and 10^{18} eV primary energy both for proton induced shower and Iron induced shower.

Considering only QGSJET-II and SIBYLL which gives very similar results, or EPOS alone, proton and Iron contours are easily distinguishable. Now comparing EPOS with the two other models, it appears clearly that EPOS has a much higher muon production rate. At 10^{18} eV for instance, there is as much muons in a proton induced shower using EPOS as in an Iron induced shower using QGSJET-II. As explain in [23], this is mostly due to the higher production of baryon/anti-baryon pair in EPOS as shown in the previous sections. A baryon not producing leading neutral pion, if there is more baryon during shower development, less energy is transferred to the electromagnetic component and hence more energy is available for muon production. Furthermore, this is related to the higher elongation rate of EPOS.

A different presentation is used in Fig.14, to show clearly that EPOS produces up to 2 times more muons than SIBYLL at 10^{21} eV for instance. To point up the primary energy dependence, the number of muons above 1 GeV reaching the ground is divided by the primary energy in GeV and plotted as a function of this energy. Then we see that in fact at low energy, the number of muons is almost the same for all the models. But the slope is different and EPOS has a slope much closer to 1, increasing the absolute number of muons, and reducing the difference between the number of muons in proton induced showers and in Iron induced showers. This will of course influence all air shower analysis based on the number of muons such as the analysis of the KASCADE experiment [30].

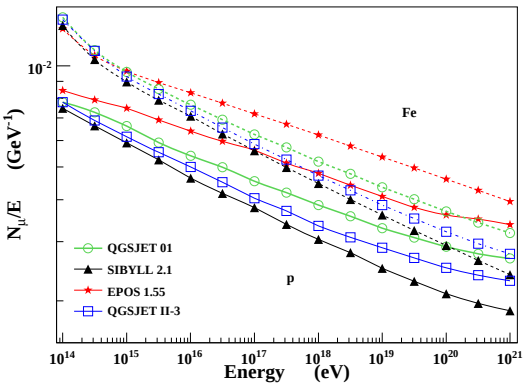

Fig. 14. Number of muons above 1 GeV at ground divided by the primary energy in GeV as a function of the primary energy in eV for different hadronic interaction models.

V. Conclusion

With the two new models, EPOS and QGSJET II, and SIBYLL 2.1, a set of three complementary models is available for air shower simulations. The models differ substantially in the approach of describing hadronic interaction data.

QGSJET II is a very sophisticated implementation of Gribov's Reggeon theory at hadron level, including soft multi-pomeron interactions. The resummation of the enhanced graphs allows one to give predictions at very high energy that depend only on a number of well-defined parameters of the underlying pomeron model. However, the resummation of all enhanced graphs is currently only possible if correlations between the individual interactions are neglected.

EPOS is an implementation of Gribov's reggeon theory at parton level. Correlations between partons in hadrons are explicitly parameterized, but within this model, the resummation of enhanced graphs is not possible. Their contribution is parameterized in vertex functions that depend on the nuclear environment (mass number, impact parameter) of the parton a Reggeon couples to. The parameterization of the vertex functions allows a nearly perfect description of existing data but introduces uncertainties in the high-energy extrapolation.

In comparison to EPOS and QGSJET II, SIBYLL 2.1 is a rather simple and straightforward model in which all assumptions are restricted to the absolute minimum needed for describing event features of relevance to air shower simulation. The extrapolation of SIBYLL mainly depends on the behaviour of the minijet cross section. Since the model

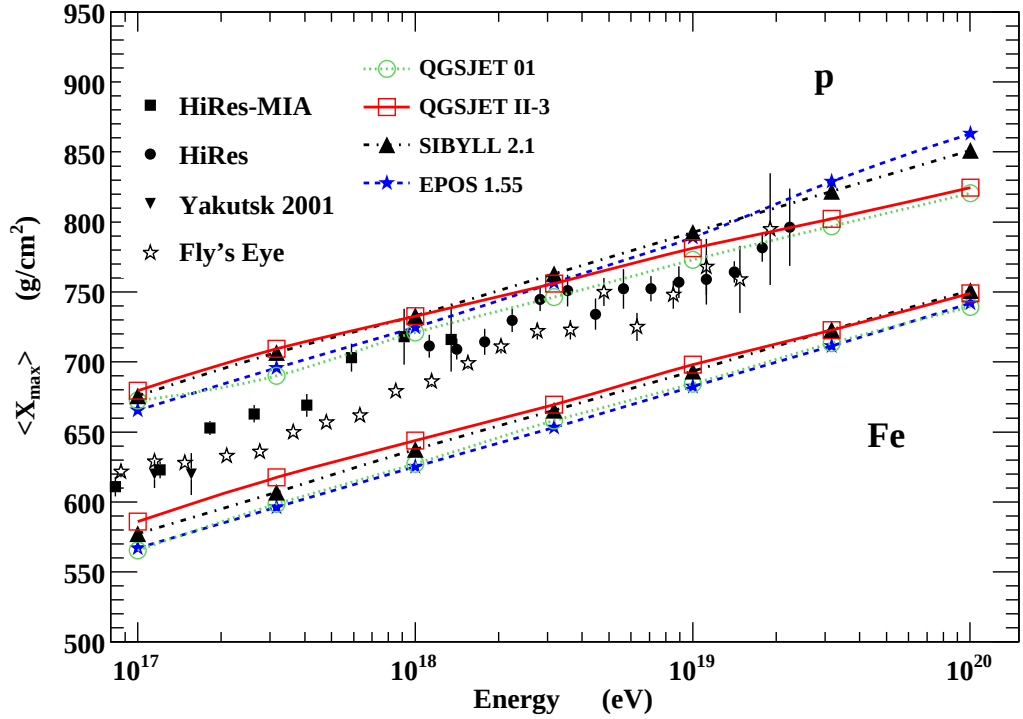

Fig. 12. Mean X_{max} for proton and Iron induced showers plotted as a function of the primary energy in eV for different high energy hadronic interaction models, together with data [31], [32], [33].

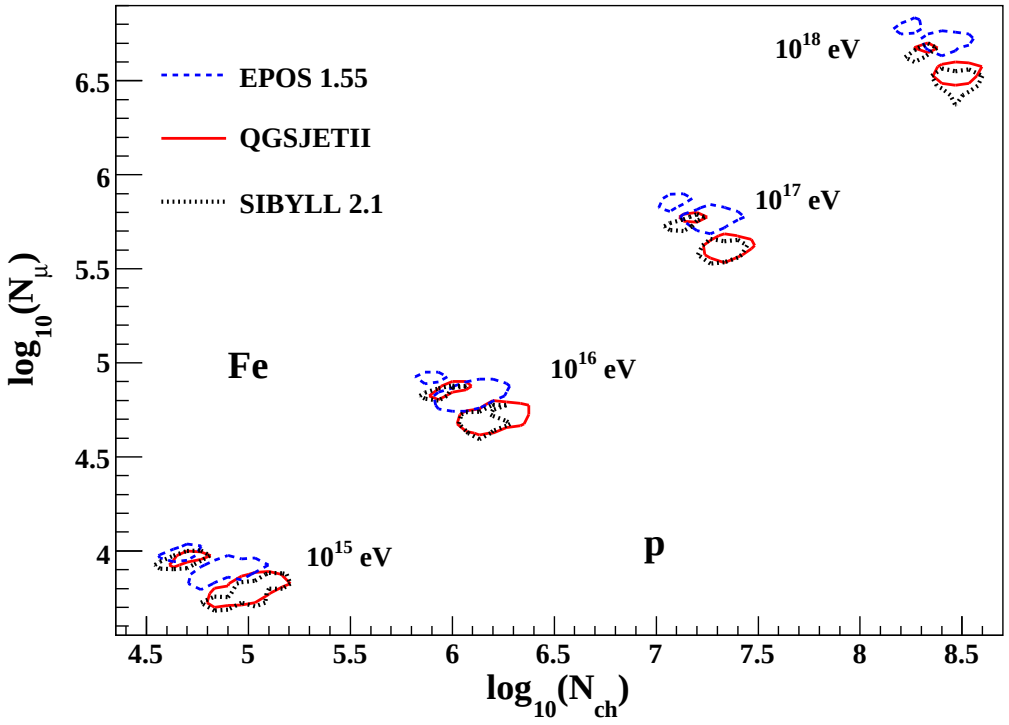

Fig. 13. Contour plot of the number of muons above 1 GeV as a function of the number of charged particles above 1 MeV at ground for proton and Iron induced showers at 10^{15}, 10^{16}, 10^{17} and 10^{18} eV for different hadronic interaction models.

does not contain an implementation of parton shadowing or saturation, the energy dependence of the minijet cross section has to be taken from an external parametrization and is rather uncertain.

Comparisons with new measurements from the RHIC Collaborations and NA49 demonstrate a reasonable overall quality of data description of currently available hadronic interaction models. However, they also provide clear indications of possible conceptional or technical shortcomings of the models. A particular challenge is the consistent description of RHIC p-p, Au-Au and d-Au data at $\sqrt{s} = 200\,\mathrm{GeV}$. Detailed studies will be needed to assess the importance of the shown discrepancies for air shower simulations. For example, in addition to the well-known role of the highest-energy secondary particles in a collision, also the multiplicity and energy distribution of baryon-antibaryon pairs, for which almost no measurements exist, is very important for the prediction of muon multiplicities in air showers.

Minimum bias measurements at LHC will help to significantly reduce the uncertainty of the extrapolation of hadronic interaction models. Proton-carbon measurements would allow model tuning without additional assumptions.

Although the presented approches to describe multiparticle production at high energy are rather different in their philosophy, a number of key elements are very similar in all models. Also, since most data available cover only the central rapidity range in collider experiments, a large part of the currently applied model concepts for hadron production is only developed for a phase space range of very limited relevance to air showers. Therefore it cannot be expected that the range of predictions shown here represents the full uncertainty of model extrapolations.

REFERENCES

[1] J. Abraham et al. (Auger Collaboration), *Nucl. Instr. Meth.* **523** (2004) 50
[2] R.S. Fletcher et al., *Phys. Rev.* **D50** (1994) 5710; R. Engel et al., *Proc. 26th Int. Cosmic Ray Conf.*, Salt Lake City (USA), **1** (1999) 415
[3] N.N. Kalmykov et al., *Nucl. Phys. B (Proc. Suppl.)* **52B** (1997) 17
[4] D. Heck et al., Report *FZKA 6019*, Forschungszentrum Karlsruhe, 1998
[5] T. Bergmann et al., *Astropart. Phys.* **26** (2007) 420
[6] S. Ostapchenko, Phys. Rev. D **74**, 014026 (2006)
[7] K. Werner, F. M. Liu and T. Pierog, Phys. Rev. C **74**, 044902 (2006) [arXiv:hep-ph/0506232].
[8] A. B. Kaidalov and K. A. Ter-Martirosian, Sov. J. Nucl. Phys. **39**, 979 (1984) [Yad. Fiz. **39**, 1545 (1984)].
[9] N. N. Kalmykov, S. S. Ostapchenko and A. I. Pavlov, Bull. Russ. Acad. Sci. Phys. **58**, 1966 (1994) [Izv. Ross. Akad. Nauk Ser. Fiz. **58N12**, 21 (1994)].
[10] F. M. Liu, H. J. Drescher, S. Ostapchenko, T. Pierog and K. Werner, J. Phys. G **28**, 2597 (2002)
[11] S. Ostapchenko, Phys. Lett. B **636**, 40 (2006)
[12] S. Ostapchenko and D.Heck, *Proc. 29th ICRC*, Pune, **7** (2005) 135.
[13] H. J. Drescher, M. Hladik, S. Ostapchenko, T. Pierog and K. Werner, Phys. Rept. **350**, 93 (2001)
[14] M. Hladik, H. J. Drescher, S. Ostapchenko, T. Pierog and K. Werner, Phys. Rev. Lett. **86**, 3506 (2001)
[15] S. S. Ostapchenko, J. Phys. G **29**, 831 (2003).
[16] F. M. Liu, J. Aichelin, M. Bleicher, H. J. Drescher, S. Ostapchenko, T. Pierog and K. Werner, Phys. Rev. D **67** (2003) 034011.
[17] C. Alt *et al.* [NA49 Collaboration], Eur. Phys. J. C **45** (2006) 343
[18] D. Barna, *PhD Thesis* NA49 Collaboration.
[19] A. E. Brenner *et al.*, Phys. Rev. D **26** (1982) 1497.
[20] C. Alt *et al.* [NA49 Collaboration], arXiv:hep-ex/0606028.
[21] D. S. Barton *et al.*, Phys. Rev. D **27** (1983) 2580.
[22] P. Grieder et al., *Proc. 13th ICRC*, Denver, **4** (1973) 2467-72.
[23] T. Pierog and K. Werner, [arXiv:astro-ph/0611311] (2006)
[24] G. Alner et al., *Phys.Rep.*, **154** (1987) 247.
[25] F. Abe *et al.* [CDF Collaboration], Phys. Rev. Lett. **61** (1988) 1819.
[26] J. Adams *et al.* [STAR Collaboration], Phys. Rev. C **70** (2004) 064907
[27] B. B. Back *et al.* [PHOBOS Collaboration], Phys. Rev. Lett. **93** (2004) 082301
[28] J. Adams *et al.* [STAR Collaboration], Phys. Lett. B **637** (2006) 161
[29] J. Matthews : Astropart. Phys. **22** (2005) 387.
[30] H. Ulrich *et al.*, Czech. J. Phys. **56** (2006) A261.
[31] T. Abu-Zayyad et al., *Astropart.Phys*, **16** (2001) 1.
[32] S. Knurenko et al., *Proc. 27th ICRC*, Hamburg, **1** (2001) 177.
[33] R.U. Abbas et al., *Astrophys. J.*, **622** (2005) 910.